J Mater Sci (2010) 45:1617–1621
DOI 10.1007/s10853-009-4137-9

Microstructure and oxidation-resistant of ZrO_2/Ni coatings applied by high-speed jet electroplating

Wei Wang · Shi Qiang Qian · Xi Ying Zhou

Received: 3 August 2009 / Accepted: 17 December 2009 / Published online: 31 December 2009

Abstract ZrO_2/Ni composite coatings with different contents of ZrO_2 particles were deposited on superalloy K17 substrate using high-speed jet electroplating process. The microhardness and microstructure of composite coatings were studied. The oxidation kinetic curves of uncoated and coated K17 alloys were obtained. The results indicated that ZrO_2/Ni composite coatings exhibit higher microhardness than that of pure nickel coatings under the same high-speed jet electrodeposition conditions. ZrO_2/Ni composite coatings exposure to air at 1000 °C for 5 h formed scale containing NiO and Cr_2O_3; after exposure to air at 1000 °C for 100 h the scale was comprised NiO, $NiCr_2O_4$, and Cr_2O_3. The formation of Cr_2O_3 scales on the ZrO_2/Ni composite coating directly improved the oxidation resistance of superalloy K17.

Introduction

The drive to improve engine combustion efficiency and reducing emissions has resulted in a significant increase of the turbine entry temperature within gas-turbine engines since 1940s. The turbine entry temperature increase has been facilitated by three principal materials developments: alloy design, casting techniques, and a viable coating technology. For the alloy design, further temperature increase is now limited by the melting point and oxidation resistance of currently used Ni-base superalloys. To overcome these limitations, Ni-base superalloy components in combustor and turbine sections are cooled by a combination of internal and surface boundary layer air cooling, and the application of an insulating surface thermal barrier coating (TBC) [1–4].

TBCs with low thermal conductivity greatly enhance operating temperatures and thermal efficiency of hot-section components in aircraft and industrial gas-turbine engines, and reduce fuel consumption and gas emissions at elevated temperatures [5–7]. Up to now, the most successful TBCs in use are based on 3.5–4.5 mol% Y_2O_3 stabilized ZrO_2, which are applied on engine components by plasma spraying [8, 9], electron-beam physical vapor deposition [10, 11], magnetron sputtering [12], and the other deposition techniques [13, 14]. These methods have been studied extensively to avoid mechanical and adherence problems between coating and substrate. Nonetheless, these techniques have some limitations, for example, industrialization is expensive and time-consuming. During recent years, interest has been generated in composite electroplating deposition of ceramic coating [15–17].

High-speed jet electroplating technique is known as a fast deposition process in copper electroplating without ceramic reinforcements [18]. During the high-speed jet electroplating, plating solution is jetted on a cathode surface directly because of the existence of electric field between the cathode and anode located in the jet stream to the cathode, the deposition takes place only on the local cathode surface area where the jet impinges on. Comparing with the conventional electrodeposition, jet electroplating possessed high depositing rate. On the other hand, the grain size refining effect of jet electroplating is more efficient since a much higher overpotential of cathodic substrate can simultaneously be used with much higher current density.

In this work, the 4-mol% Y_2O_3 stabilized ZrO_2/Ni composite coatings were deposited by high-speed jet

W. Wang (✉) · S. Q. Qian · X. Y. Zhou
School of Materials Engineering, Shanghai University of Engineering Science, No. 333 Longteng Road, 201620 Shanghai, People's Republic of China
e-mail: wangwei200173@sina.com

electroplating technique. The isothermal oxidation behavior of the ZrO_2/Ni composite coatings at 1000 °C was investigated.

Experimental

The cast K17 superalloy was used as substrate material. Specimens in the form of plates with dimension of 2 mm × 10 mm × 20 mm were cut and polished to a mirror finish with 1-μm Al_2O_3 power, then degreased by detergent and further ultrasonically cleaned in deionized water and acetone, then dried by N_2 gas. As an incorporated ceramic reinforcement, the 4-mol% Y_2O_3 partially stabilized ZrO_2 particles with an average diameter of 30–40 nm were supplied.

ZrO_2/Ni composite coatings were prepared through co-depositing ZrO_2 particles and pure nickel on the superalloy substrate by high-speed jet electroplating technique. Before jet electroplating, a mechanical method, ultrasonic, and surfactant (MZS) were used to make ZrO_2 particles to be uniformly suspended in a nickel jet electroplating electrolyte as soon as possible. The composition of the high-speed jet electroplating electrolyte was as follows: 260 g/L $NiSO_4 \cdot 6H_2O$, 50 g/L $(NH_4)_3C_6H_5O_7$, 150 g/L ammonia and 200–1200 wt ppm ZrO_2. The temperature of the jet electroplating bath was kept at 45 °C at pH 7. The jet speed, scanning jet speed, jet voltage, and jet time were 360 L/h, 6 mm/s, 8 V, and 15 min, respectively. The isothermal oxidation was performed on a muffle stove in static air, and the weight changes were measured discontinuously and the parabolic rate constants were calculated afterward. The weight of each sample was determined using an electrobalance with a detection limit of 0.01 mg during the isothermal oxidation. The cast alloy and composite coatings were oxidized isothermally at 1000 °C for 100 h in air.

The structures and the morphologies of coatings and oxide scales were characterized by X-ray diffraction (XRD) and scanning electron microscopy (SEM). The Vickers microhardness was measured by microhardness tester (HX-1000) with a load of 100 g for 15 s.

Results and discussions

The surface images of the coatings analyzed by SEM were given in Fig. 1. It can be indicated that the surface of high-speed jet electroplating nickel coating is rather rough with bulky and irregular nodular units (Fig. 1a), whereas the surface of high-speed jet electroplating ZrO_2/Ni composite coating characterizes small nodular, smooth, and uniform units (Fig. 1b). The change in the morphology can be associated to the change from preferred orientation to random-oriented composite. In addition, many nodular agglomerated grains are seen on the ZrO_2/Ni composite coating surface. It is supposed that the ZrO_2 particulates of a uniform distribution and agglomeration to some extent may contribute to increase the microhardness of the ZrO_2/Ni composite coating.

Figure 2 showed the variation in the microhardness of high-speed jet electroplating ZrO_2/Ni composite coatings with the content of ZrO_2 particulates. It can be seen that the microhardness of composite coatings increases with increasing the content of ZrO_2 particulates. The increase in the microhardness of ZrO_2/Ni composite coatings as compared to nickel coating is rationally understood, since ZrO_2 particulates deposited in the nickel matrix could restrain the growth of the nickel grains and the plastic deformation of the matrix under a loading, by way of grain refining and dispersive strengthening effects become stronger with increasing ZrO_2 particulates content; thus, the microhardness of ZrO_2/Ni composite coatings increase with increasing ZrO_2 particulates content.

Figure 3 showed the oxidation kinetics curves of ZrO_2/Ni composite coatings for different ZrO_2 content and superalloy K17 exposure in air at 1000 °C for 100 h. It shows that the weight gains are obvious in the early

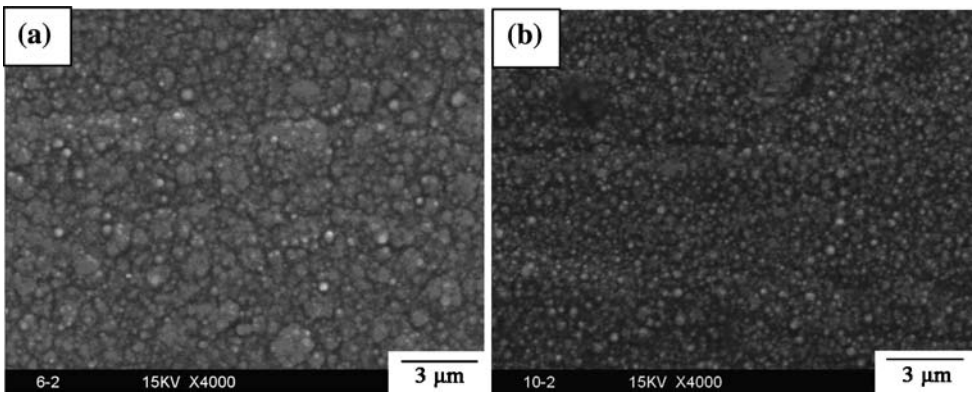

Fig. 1 SEM images of surface images of high-speed jet electroplating **a** nickel coating and **b** ZrO_2/Ni composite coating

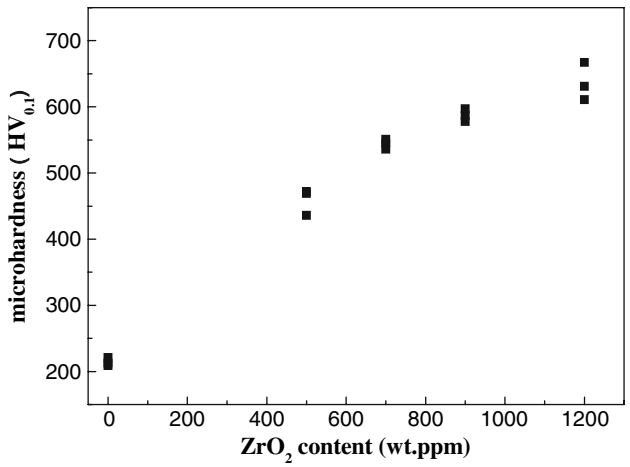

Fig. 2 Change in the microhardness of composite coatings as a function of ZrO_2 content

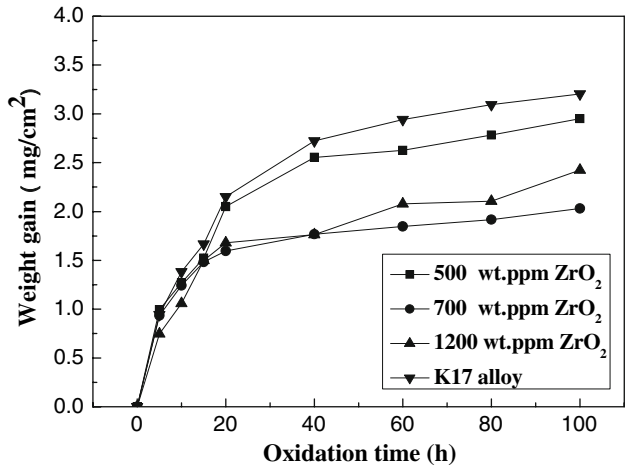

Fig. 3 Isothermal oxidation kinetic curves of ZrO_2/Ni composite coatings for different ZrO_2 content and superalloy K17 at 1000 °C for 100 h

oxidation stage and no great change was found 20 h later. It can be seen that the weight gains of ZrO_2 content for 700 wt ppm are smallest after 100 h oxidation, while the weight gain of uncoated K17 alloy is the greatest among the samples. These evidences show that ZrO_2/Ni composite coatings blocked the oxidation and protected the superalloy K17 effectively.

SEM images of ZrO_2 (700 wt ppm)/Ni composite coatings after the isothermal oxidation at 1000 °C for 5 and 100 h in air are given in Fig. 4a and b, respectively. It can be seen that oxides formed after isothermal oxidation at 1000 °C for 5 h are a mixture of small round grains and some faced nodules (Fig. 4a). It can also be seen that the morphologies of the oxides formed after isothermal oxidation at 1000 °C for 100 h are continuous and dense (Fig. 4b), whereas microstructures of oxides formed after the isothermal oxidation at 1000 °C for 5 h are porous, indicating that the oxide film of specimens after oxidation at 1000 °C for 5 h is not protective enough.

Figure 5 showed the cross-sectional SEM images of ZrO_2 (700 wt ppm)/Ni composite coatings after the isothermal oxidation at 1000 °C for 5 and 100 h in air, respectively. SEM examination on cross sections revealed that the formed oxide scales become thicker (from ~15 μm for 5 h duration to ~50 μm for 100 h duration) with increasing the isothermal oxidation duration at 1000 °C.

To identify the phases developed on the surface of ZrO_2 (700 wt ppm)/Ni composite coatings after isothermal oxidation at 1000 °C for 5 and 100 h, the specimen surfaces were analyzed by X-ray diffraction. The results are shown in Fig. 6. For the oxidation of ZrO_2 (700 wt ppm)/Ni composite coatings after isothermal oxidation at 1000 °C for 5 h, XRD shows strong peaks of NiO and very weaker peaks of Cr_2O_3 (Fig. 6a). For the oxidation of ZrO_2 (700 wt ppm)/Ni composite coatings after isothermal oxidation at 1000 °C for 100 h, it can be seen from Fig. 6b that the main oxides on the surface of ZrO_2 (700 wt ppm)/Ni composite coatings are composed of NiO, $NiCr_2O_4$, and Cr_2O_3.

Generally, the high temperature oxidation resistance of superalloys depends on the stability of oxides of Cr and Zr on the surface, because both metal and oxygen atoms have low diffusion coefficients in these oxides [3]. When

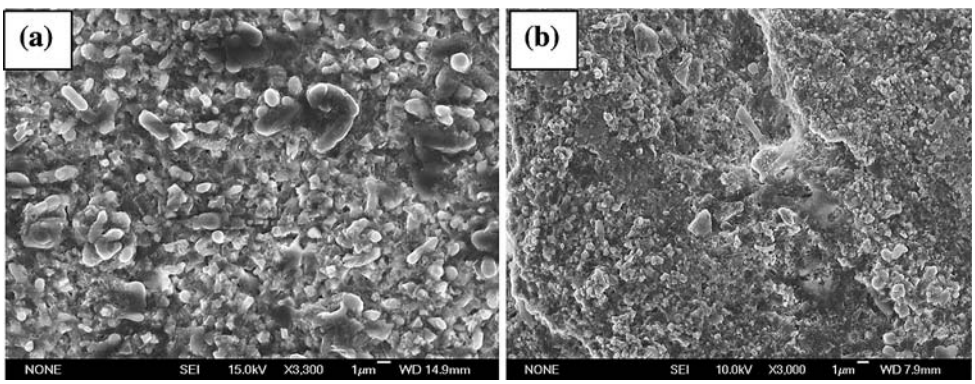

Fig. 4 SEM images of ZrO_2 (700 wt ppm)/Ni composite coatings after the isothermal oxidation at 1000 °C in air for **a** 5 h and **b** 100 h

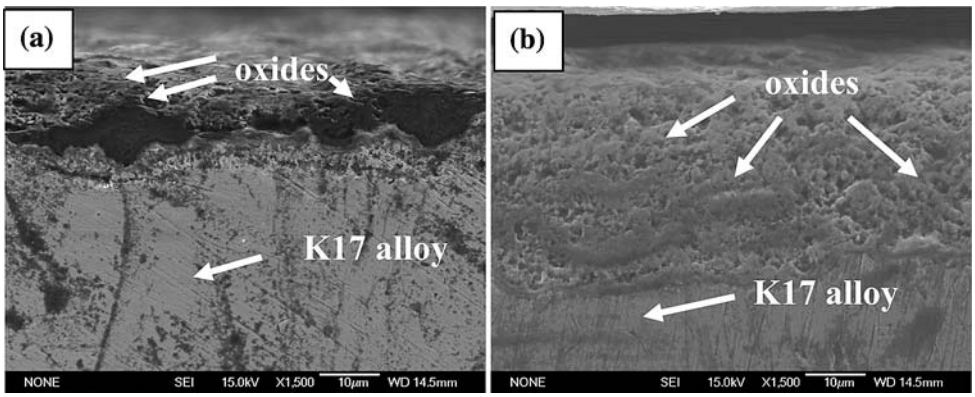

Fig. 5 Cross-sectional SEM images of ZrO_2 (700 wt ppm)/Ni composite coatings after the isothermal oxidation at 1000 °C in air for **a** 5 h and **b** 100 h

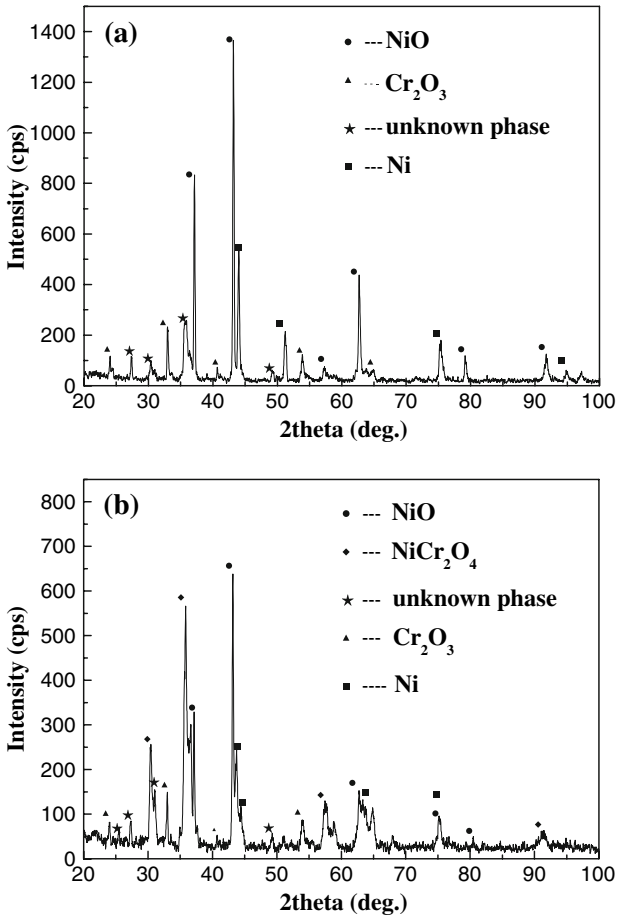

Fig. 6 XRD patterns for ZrO_2 (700 wt ppm)/Ni composite coatings after exposure in air at 1000 °C for **a** 5 h and **b** 100 h

homogeneous and stable scales cover the surface, excellent oxidation resistance is obtained. While spinel-type oxides, such as NiO and $NiCr_2O_4$, are not better oxidation resistance at high temperature [19]. In this experiment, ZrO_2 and Cr_2O_3 covered the surface when the specimens were exposed at 1000 °C. As a result, high temperature oxidation resistance of superalloy K17 was obviously improved by coating with ZrO_2/Ni composite coatings.

Conclusions

High-speed jet electroplating the 4-mol% Y_2O_3 stabilized ZrO_2/Ni composite coatings on K17 superalloy had been successfully deposited. Through isothermal oxidation tests, SEM and XRD analysis, several conclusions were drawn.

Microhardness and ZrO_2 particles content of the 4-mol% Y_2O_3 stabilized ZrO_2/Ni composite coatings are greatly affected by high-speed jet electroplating process. ZrO_2/Ni composite coatings exhibited higher microhardness than that of pure nickel coatings which were prepared under the same electrodeposition conditions.

After the ZrO_2/Ni composite coatings were deposited, the scales mainly contained NiO and Cr_2O_3 exposure at 1000 °C for 5 h; NiO, $NiCr_2O_4$, and Cr_2O_3 at 1000 °C for 100 h. The formation of Cr_2O_3 scales on the ZrO_2/Ni composite coating directly improved the oxidation resistance of alloy K17.

Acknowledgements This work is supported by the Shanghai Municipal Developing Foundation of Science &Technology under Grant 0852nm01400.

References

1. Wang YQ, Sayre G (2009) Surf Coat Technol 203:2186
2. Lee JH, Tsai PC, Lee JW (2009) Thin Solid Films 517:5253
3. Kakuda TR, Limarga AM, Bennett TD, Clarke DR (2009) Acta Mater 57:2583
4. Varanasi VG, Besmann TM, Hyde RL, Payzant EA, Anderson TJ (2009) J Alloy Compd 470:354
5. An K, Han MK (2006) J Mater Sci 41:2113. doi:10.1007/s10853-006-3144-3
6. Pint BA, More KL (2009) J Mater Sci 44:1676. doi:10.1007/s10853-008-3221-x
7. Théry PY, Poulain M, Dupeux M (2009) J Mater Sci 44:1726. doi:10.1007/s10853-008-3108-x
8. Mishra SB, Chandra K, Prakash S (2008) Mater Lett 62:1999
9. Singh H, Puri D, Prakash S (2005) Surf Coat Technol 192:27
10. Théry PY, Poulain M, Dupeux M, Braccini M (2007) Surf Coat Technol 202:648
11. Vecchione N, Wasmer K, Balint DS, Nikbin K (2009) Surf Coat Technol 203:1743

12. Ren X, Wang FH (2006) Surf Coat Technol 201:30
13. Krishnaveni K, Narayanan TSNS, Seshadri SK (2009) J Mater Sci 44:433. doi:10.1007/s10853-008-3135-7
14. Hattori T, Kaneko Y, Hashimoto S (2008) J Mater Sci 43:3923. doi:10.1007/s10853-007-2372-5
15. Biest OVD, Joos E, Vleugels J (2006) J Mater Sci 41:8086. doi:10.1007/s10853-006-0635-1
16. Aal AA (2008) J Mater Sci 43:2947. doi:10.1007/s10853-007-1796-2
17. Jung A, Natter H, Hempelmann R et al (2009) J Mater Sci 44:2725. doi:10.1007/s10853-009-3330-1
18. Takeuchi H, Tamura S, Tsunekawa Y, Okumiya M (2004) Surf Eng 20:25
19. Wang B, Sun C, Gong J, Huang RF, Wen L (2004) Corros Sci 46:519